PROGRESS IN MRI FE-RESONANCE/RAYLEIGH/MIE DOPPLER LIDAR

Xinzhao Chu[1], Wentao Huang[1], Jeffrey P. Thayer[1], Zhangjun Wang[1], and John A. Smith[1]

[1]*University of Colorado at Boulder, 216 UCB, CIRES, Boulder, CO 80309, USA, Email: Xinzhao.Chu@Colorado.edu*

ABSTRACT

Ambitiously aiming to achieve bias-free resonance Doppler lidar for advancing the middle and upper atmosphere physics and chemistry, we started the development of a Major Research Instrumentation (MRI) mobile Fe-resonance/Rayleigh/Mie Doppler lidar about two years ago at the University of Colorado at Boulder. We report the significant progress made in the last two years, especially on the revolutionary ideas of pulsed alexandrite ring laser, Fe Doppler-free spectroscopy, and optical heterodyne detection for accurate frequency control and spectral analysis of the lidar pulse. Substantial efforts have also been spent to construct large-aperture receiver, state-of-the-art data acquisition and control system, and mobile lidar laboratory. We introduce the overall lidar architecture to inspire future lidar advancement worldwide.

1. INTRODUCTION

To push the middle and upper atmosphere science to a new level, it is crucial to make global lidar observations with unprecedented accuracy, precision, and resolution. Accuracy of ~0.1 K and 1 cm/s is required for new science endeavors. Due to various factors like chirp and saturation, current state-of-the-art resonance Doppler lidars provide ~1 K and 1 m/s precision with a few K and m/s inaccuracy [1]. We proposed and then were funded by the National Science Foundation to develop a Major Research Instrumentation (MRI) mobile Fe-resonance/Rayleigh/Mie Doppler lidar in order to meet these challenges [2, 3]. The choice of Fe Doppler lidar came from the combination of high Fe abundance, short UV 372-nm wavelength, high temperature and wind sensitivity, deep Fraunhofer line in solar spectrum, and solid-state laser technologies. Besides integrating the proven 3-frequency Doppler lidar technology with large-aperture receiver and modern data acquisition, we spent tremendous efforts to develop a unique pulsed alexandrite ring laser and revolutionary approaches to achieve a single-frequency high-power all-solid-state lidar transmitter with accurate absolute-frequency calibration and chirp-free frequency stabilization of each lidar pulse. This opens the door for bias-free and high-accuracy wind and temperature measurements. Below we introduce the progress made so far and point out the potentials of several new technologies produced.

2. ARCHITECTURE OF MRI DOPPLER LIDAR

A major philosophy behind the MRI lidar design is to control and monitor the laser pulse frequency and spectrum, rather than only controlling the cw seed laser frequency. Stabilizing the PARL laser frequency directly onto the peak of Fe 372-nm absorption line will remove the uncertainty in chirp-induced laser pulse frequency error. Thus, we could achieve the highest accuracy, leading to bias-free measurements of wind and temperature. Another key point is to make the lidar system, especially the transmitter lasers, as stable as possible. Stability is the basis of any meaningful calibration for sophisticated science studies like long-term trends and accurate temperature and wind. The laser system must be developed in a robust way to fight against the harsh environment during remote and mobile deployment. The third major thought is to seek high laser power, large receiving aperture, and high detection efficiency for acquiring high precision and resolution measurements. We designed the entire lidar system based on these ideas, and we are developing the lidar by creating new approaches and integrating the latest advanced technologies into the system.

A schematic diagram of the entire MRI Doppler lidar is illustrated in Figure 1. It consists of three major systems: the lidar transmitter, the lidar receiver, and the data acquisition & control system. This MRI lidar is based on the injection-seeded frequency-doubled Pulsed Alexandrite Ring Laser (PARL) technology to detect neutral Fe atoms in the mesosphere and lower thermosphere via the Fe 372-nm absorption line. A single-frequency continuous-wave (cw) External Cavity Diode Laser (ECDL) operating at 744 nm provides the seeding source. It is locked to the double wavelength of the Fe 372-nm peak via a reference cavity. The two wing frequencies needed are generated with dual acousto-optic frequency shifters [1]. Through probing the Doppler shifted and broadened Fe spectroscopy at three preset frequencies (peak and two wings), the line-of-sight (LOS) wind and temperature are inferred simultaneously along with Fe density and aerosol/cloud signals [3]. The lidar beam is pointed to zenith, north, and east (ZNE) sequentially or split to three beams pointing to ZNE simultaneously. Return photons from ZNE are collected by three large-aperture telescopes and detected by receiver chains. Using such a Doppler-Beam-Swing technique, we derive the vector wind from three measured LOS wind components. New approaches have been taken to monitor and control the laser temporal, spatial and spectral characteristics. A data acquisition and control system utilizing modern computing technologies helps accomplish the tasks and synchronize between the transmitter and receiver.

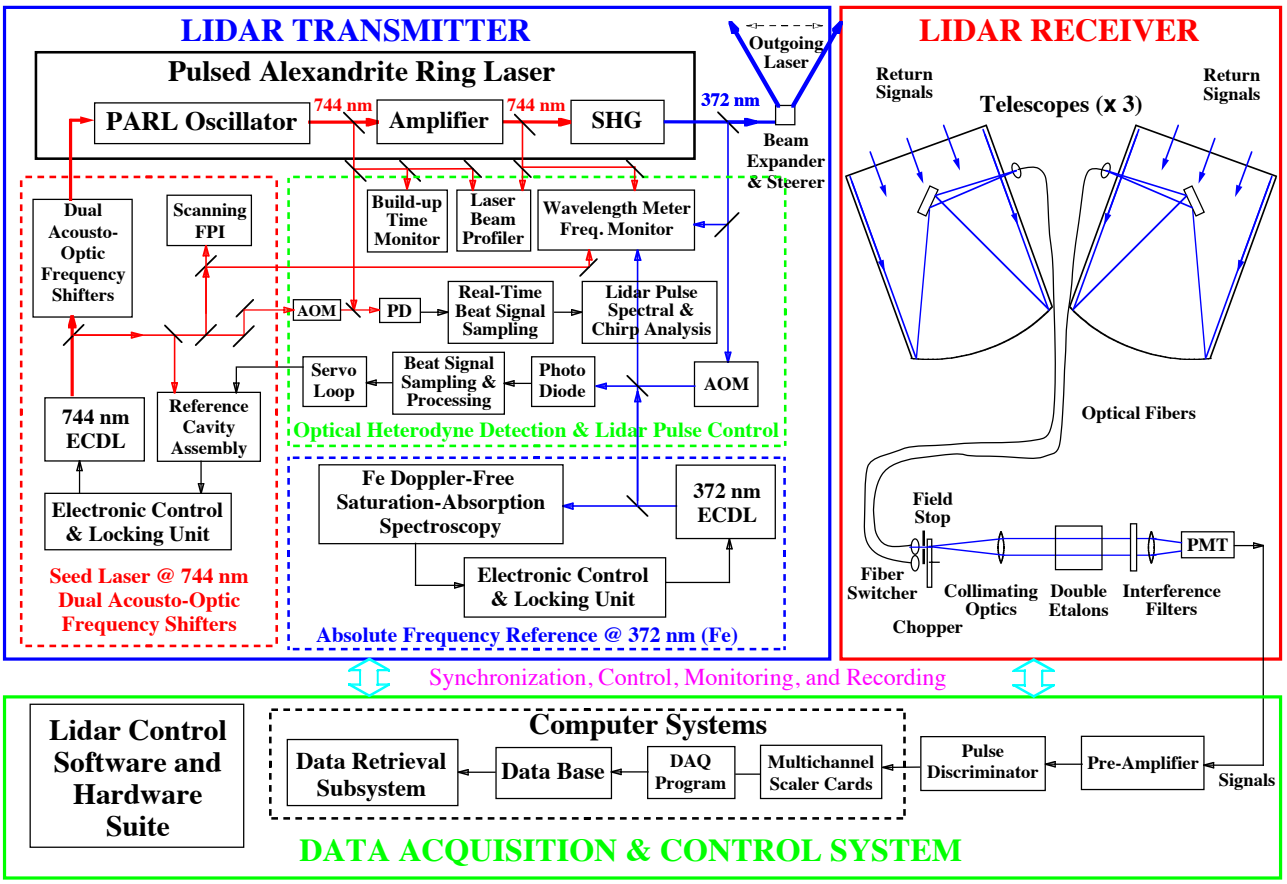

Figure 1. Architecture of the MRI Mobile Fe-resonance/Rayleigh/Mie Doppler lidar.

2.1. PARL Frequency Control & Calibration

Alexandrite (Cr^{3+}:$BeAl_2O_4$) laser developed by Walling and co-workers [4] is a solid-state tunable laser whose fundamental wavelength covers 700-818 nm with the gain peak centered around 750 nm. Combining with nonlinear optics such as frequency doubling and tripling as well as Raman shift, alexandrite laser can cover from UV to IR range, therefore, very attractive to high-precision spectroscopy and resonance lidar fields. In fact, Fe and K lidars based on alexandrite lasers have been used to measure temperature in MLT region [5-7]. Several excellent properties of alexandrite gain medium make it an ideal candidate for achieving single-frequency and high-energy lidar pulses. To achieve single-mode and single-frequency alexandrite laser, a ring cavity for traveling wave must be constructed to avoid spatial-hole burning. Unlike the dye ring laser with a folded cavity of curvature mirrors, a PARL cavity is formed with four flat mirrors in a rectangular arrangement. Further steps must be taken to select single longitudinal mode from the PARL oscillator.

The most effective approach is to injection seed the PARL oscillator with a single-frequency cw seed laser. Injection seeding technology relies on the regenerative amplification of seed laser inside the PARL oscillator to generate seeding fringes, and then firing Q-switch when the oscillator cavity is in exact resonance with the seed laser frequency. The seed laser helps a single cavity mode to build up much faster than other modes, thus eliminating other modes through mode competition in homogeneously broadened gain medium. To ensure reliable injection seeding, several distinct approaches haven emerged, such as build-up reduction, active cavity length stabilization, Pound-Drever-Hall locking, ramp-fire, ramp-hold-fire, and ramp-delay-fire, etc.

With an original idea proposed by Dr. Xinzhao Chu of University of Colorado, Dr. John Walling of Light Age, Inc. developed a novel ramp-fire technology to ensure reliable injection seeding to PARL oscillator while compensating the chirp effect in the pulsed laser. To meet the specifications required by this MRI Doppler lidar, a configuration of "oscillator + amplifier + second harmonic generation" (Figure 1) is used in the PARL system to achieve high-energy but still single-frequency laser pulses at UV 372-nm. An oscillator with a long resonator length (~3 m) is constructed to enlarge the beam diameter inside the laser rod, allowing the same energy extraction from the laser rod at lower energy

density. This helps lowering the chirp and also helps increasing the pulse width (~300 ns) to avoid the Fe-layer saturation effect in MLT region.

Frequency chirp refers to the discrepancy between the central frequency of the laser pulse and the seed laser frequency. It is produced because the refraction index *n* of the laser rod is gain-dependent so reduces during the laser pulse's build-up. Although the injection seeding helps select single longitudinal mode to lase, the actual output laser frequency is still determined by the oscillator cavity resonance frequency. With a changing optical cavity length caused by *n* change, the laser pulse changes its frequency throughout the pulse width. This not only leads to an offset in the pulse central frequency, but also broadens the pulse spectral width. The uncontrolled and varied chirp is a leading error source that prevents current Na, K, and Fe Doppler lidar from achieving better than 1-K and 1-m/s accuracy.

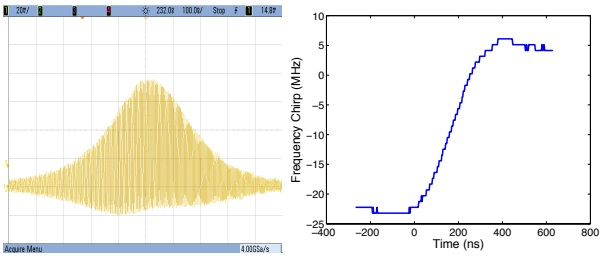

Figure 2. Optical beat signal obtained with PARL and ECDL (left) and inferred frequency chirp of the PARL pulse (right).

To monitor the PARL chirp, we introduce the optical heterodyne detection (OHD) into resonance lidar for the first time. This is based on an earlier proposal for PDA chirp study [1] and inspired by coherent Doppler lidar. As shown in Figure 1, a small portion of the seed laser is frequency shifted by 240 MHz via an acousto-optic modulator (AOM). The shifted cw beam is mixed with a tiny portion of the PARL pulse at a fast photodiode. The beat signal is detected and sampled to a 4-GSa/s fast oscilloscope (Figure 2a). Fourier analysis of the beat signal exhibits varying pulse frequency throughout the entire pulse duration (Figure 2b). The overall edge-to-edge spectral linewidth is ~30 MHz for the PARL oscillator at its fundamental wavelength 744 nm.

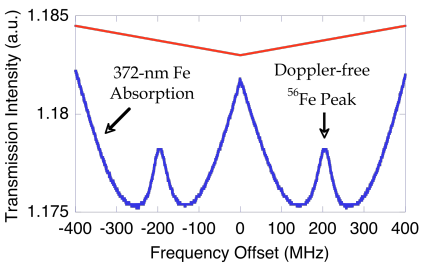

Figure 3. Fe Doppler-free saturation-absorption spectroscopy obtained the MRI lidar at Fe 372-nm line.

To remove chirp influence on measurement accuracy, our revolutionary idea is to lock the lidar pulse frequency directly onto the Fe 372-nm line peak. First, a 372-nm ECDL is locked to the peak of Fe Doppler-free saturation-absorption spectroscopy at 372 nm (Figure 3) via modified Pound-Drever-Hall technology, thus transferring the absolute frequency reference from the Fe line to the 372-nm ECDL. Second, we apply the optical heterodyne detection technique to the 372-nm cw and pulsed lasers (Figure 1). The beat signal tells whether the 372-nm pulse frequency differs from the Fe peak. If discrepancy occurs, we then tune the PARL frequency via the 744-nm seed laser to make the lidar pulse frequency match the absolute frequency reference. Such scheme is expected to produce a bias-free Doppler lidar for the first time in the world. Details are given in a separate ILRC paper by *Chu and Huang* [8].

2.2. Lidar Receiver System

The MRI lidar receiver will ultimately consist of three telescopes pointing to zenith, north, and east directions in order to resolve vector wind measurements. One of the telescopes has been assembled and tested in Boulder (Figure 4). The nominal off-zenith angle is 35 degrees, and this angle can be varied according to measurement needs. This is a Newtonian-Dobsonian telescope with diameter of 0.812 m and F/number of 2.21. The primary and secondary mirrors have reflectivity of 88%. The pointing stability of the telescope is better than 0.1 degree, and steering repeatability is 559 μrad. Two optical encoders are mounted on the azimuth and altitude axis of the telescope to register angular motion in those two orthogonal planes. A double-etalon will be added in the lidar receiver as a narrowband filter to assist daytime measurements.

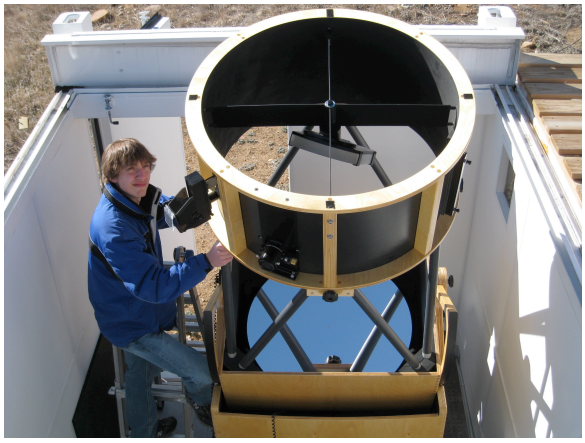

Figure 4. An 80-cm Newtonian telescope of the MRI lidar in the receiver container with the large hatch fully open.

2.3. Data Acquisition and Control System

The architecture of the data acquisition and control system is shown in Figure 5. It consists of a lidar system

control suite, a data acquisition subsystem, a data storage base, and a data retrieval program, plus a display module. The DAQ and control programs are LabVIEW-based software system, while the data retrieval is written in MatLab code. We try to control, monitor and record every system parameter while keeping the user interface as friendly as possible. The MRI DAQ program has been tested in field campaigns with a Na Doppler lidar.

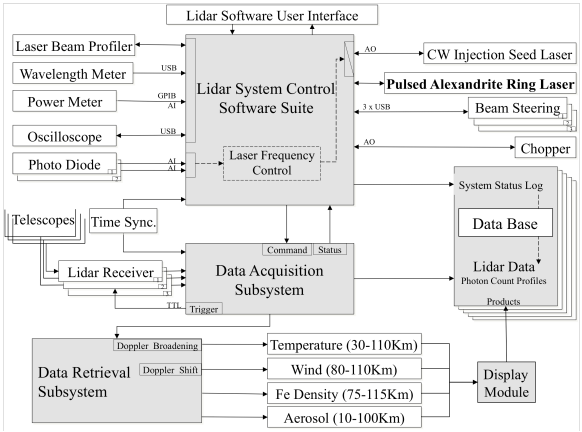

Figure 5. Architecture of the overall data acquisition and control system for the MRI Fe Doppler lidar.

3. INSTRUMENTATION FOR MOBILE DEPLOYMENT

The MRI lidar is designed to be robust and compact for ground-based or seaborne mobile deployment. It is containerized to move with a truck or ship to field locations of interest with extensive geographic coverage. Displayed in Figure 6 are the mobile lidar containers sitting at the Table Mountain Lidar Observatory in Boulder, Colorado. The container on the left hosts the lidar transmitter and the receiver detection chains, while the one on the right with a large movable hatch houses three telescopes pointing to zenith, north and east. Many designs are based on the experiences and lessons learned from the previous deployment of containerized Fe Boltzmann lidar at Rothera, Antarctica.

Figure 6. Mobile lidar laboratory consisting of two containers that host the MRI Fe Doppler lidar for mobile deployment.

4. CONCLUSIONS

The MRI mobile Fe-resonance/Rayleigh/Mie Doppler lidar integrates revolutionary ideas and state-of-the-art technologies to push lidar science forward. This lidar will provide simultaneous bias-free measurements of temperature (30-110 km), wind (75-110 km), Fe density (75-115 km), and aerosol (10-100 km) in both day and night with high accuracy, precision, and spatial and temporal resolutions. An attractive while very challenging measurement – the vertical drift associated with the residual meridional circulation (requiring a few cm/s accuracy) may be within the reach of this lidar. The ideas of OHD and lidar pulse frequency control developed here can be readily applied to other lidars.

ACKNOWLEDGEMENTS

We sincerely acknowledge John C. Walling and his colleagues at Light Age, Inc. for their superb efforts in PARL development. We thank J. S. Friedman, J. Wiig, A. Brown, N. Bradley, M. Hayman, and W. Fong for their contributions. We are grateful to Mike Hardesty, Chiao-Yao She and Chester S. Gardner for their inspiration and advice. This project is supported by NSF MRI Award ATM-0723229. XC, WH and JPT were partially supported by NSF CRRL ATM-0545353. ZW and JAS respectively acknowledge the generous support from Chinese Scholarship Council and NASA Earth and Space Science Fellowship (NNX09AO35H).

REFERENCES

[1] Chu, X., and G. Papen, Resonance fluorescence lidar for measurements of the middle and upper atmosphere, *Laser Remote Sensing*, ed. Fujii and Fukuchi, CRC Press, ISBN: 0-8247-4256-7, pp. 179-432, 2005.

[2] Chu, X., Alexandrite-ring-laser-based Fe Doppler lidar for mobile/airborne deployment, *Proc. 23rd ILRC*, 385-388, Nara, Japan, 24-28 July 2006.

[3] Chu, X., W. Huang, J. S. Friedman, and J. P. Thayer, MRI: Mobile Fe-Resonance/Rayleigh/Mie Doppler lidar principle, design, and analysis, *Proc. 24th ILRC*, pp. 801-804, Boulder, CO, 23-27 June 2008.

[4] Walling, J. C., et al., *IEEE J. Quantum Electron. QE-16,* 1302–1315, 1980.

[5] Chu, X., et al., Fe Boltzmann temperature lidar: Design, error analysis, and initial results at the North and South Poles, *Appl. Opt., 41*, 4400-4410, 2002.

[6] von Zahn, U., and J. Höffner, Mesopause temperature profiling by potassium lidar, *Geophys. Res. Lett.*, *23*, 141-144, 1996.

[7] Lautenbach, J., and J. Höffner, Scanning iron temperature lidar for mesopause temperature observation, *Appl. Opt., 43*, 4559-4563, 2004.

[8] Chu, X., and W. Huang, Fe Doppler-free spectroscopy and optical heterodyne detection for accurate frequency control of Fe-resonance Doppler lidar, *Proc. 25th ILRC*, St. Petersburg, Russia, 2010.